Structure, Dynamic Properties, and Surface Behavior of Nanostructured Ionomeric Polyurethanes from Reactive Polyhedral Oligomeric Silsesquioxanes

Stefano Turri* and Marinella Levi

Department of Chemistry, Materials and Chemical Engineering "Giulio Natta", Politecnico di Milano, Piazza Leonardo da Vinci 32, 20133 Milan, Italy

Received December 29, 2004; Revised Manuscript Received April 11, 2005

ABSTRACT: A series of linear ionomeric polyurethanes were synthesized and obtained as stable aqueous dispersions using various amounts (ca. 6−20%) of a diol functionalized polyhedral oligomeric silsesquioxane (POSS) comonomer. Polymers were characterized by GPC, XRD, DSC, dynamic rheology, and contact angle measurements. POSS macromonomers can be easily copolymerized, giving stable aqueous dispersions if the POSS content is ≤10%. The X-ray diffraction analysis of cast films showed the presence of residual crystallinity even at the lowest nanofiller dosage. Dynamic mechanical analysis showed a reinforcement effect mainly when longer soft segments (poly(tetramethylene glycol) 2000) were used. Contact angle measurements indicated a significant surface hydrophobicity enhancement as well as reduction in surface energy components calculated according to the harmonic mean approximation.

Introduction

Reactive polyhedral oligomeric silsesquioxanes (POSS) are functional nanoscale fillers consisting of an eight-corner, $-(SiO_{1.5})_n$-based cage bearing one or more functional groups.[1−6] They represent an interesting class of precursors for the synthesis of molecularly designed organic−inorganic hybrids. In fact, chemical reactivity and self-assembling properties of POSS structures make it feasible the realization of nanostructured materials following a classical bottom-up approach: recently, these systems were classified as zero-D nanocomposites.[7] In the past years reactive POSS have been grafted or copolymerized in a variety of polymeric materials including styrenics,[8−13] acrylics,[14−17] epoxies,[18−23] polyolefins,[24−28] polyimides,[29,30] and others. Their unique feature is related to the feasibility of chemical modification of many macromolecular substances at the molecular level. In this sense the resulting materials are quite different from more conventional polymeric nanocomposites, like those realized from layered phyllosilicates or metal oxide nanoparticles, since the POSS cage may be in most cases chemically linked to the matrix polymer.

Despite the growing number of scientific and patent literature, there are few cases of POSS practical exploitation,[31−33] also because their cost is still high. Generally, a higher thermal stability, a better environmental durability in special conditions (i.e., exposure to atomic oxygen and fire resistance), and, in some cases, an improvement in mechanical properties (reinforcement) are expected for POSS modified polymers.[34−36]

A special field is represented by POSS-modified polyurethanes[37] (PU) because these polymers encompass a huge number of specialized applications. Some papers have appeared in recent years about synthesis, morphological characterization, and deformation behavior of POSS-modified thermoplastic PU elastomers.[38−40] In this paper some results about preparation, dynamic properties, and surface behavior of a series of model POSS-modified ionomeric polyurethane aqueous dispersions are reported. As known, waterborne PU are increasingly used as high-performance coating systems.[41] Besides the interest in the investigation of structure to property relations of a new family of polymeric materials, we believe that many features of POSS-based polymers like improved reaction to fire and resistance to atomic oxygen as well as the possibility to build nanostructured surfaces may be exploited in the field of surface coating for specialized applications.

Experimental Part

Materials. Poly(tetramethylene glycol) (PTMG, M_n 1000 and 2000) and dimethylolpropionic acid (DMPA) were dried (80°, 1 mmHg, 8 h) before use. Isophorone diisocyanate (IPDI), triethylamine (TEA), and ethylenediamine (EDA) were used as received. *N*-Methylpyrrolidone (NMP) was stored over dry molecular sieves before use. All these reagents and solvents were purchased by Aldrich. TMP-diolisobutyl-POSS (in the following POSS-diol, from Hybrid Plastics) was used as received. The chemical structure of reagents used is shown in Scheme 1.

The reference prepolymer was synthesized by dissolving PTMG, DMPA, TEA (with $COOH/NR_3 = 1$ M), and IPDI (NCO/OH = 2 M) in NMP (15% w/w), in an agitated vessel kept under N_2. The reaction mixture was catalyzed with dibutyltin dilaurate (DBTDL, 0.1% w/w on IPDI), and conversion of reaction was monitored through chemical titration according to the classical dibutylamine/HCl method. Once the prepolymer was formed, it was poured into a beaker containing EDA ($NH_2/NCO = 0.90$) and water kept at about +5 °C, agitated with a turbine impeller working at 100 rpm. Polymerization conversion was checked by FTIR spectroscopy by monitoring the disappearance of the NCO band at 2260 cm^{-1}. POSS-modified polyurethanes were prepared in the same way, except for the fact that various amounts (about 6−20% w/w, see Table 1) of POSS macromonomer were added in the prepolymerization step; stoichiometric ratios of chain extension step were accordingly corrected in order to keep the NH_2/NCO stoichiometric ratio = 0.90 in all cases. In all polyurethanes synthesized the DMPA content was 3.0 ± 0.2 wt %. The resulting stable, milky aqueous dispersions (solid content 30 ± 1%) of the ionomeric polyurethanes were cast on different substrates

* Corresponding author: e-mail stefano.turri@polimi.it, tel +39 (0) 223993252.

10.1021/ma047304g CCC: $30.25
Published on Web 05/27/2005

Scheme 1. Simplified Reaction Scheme

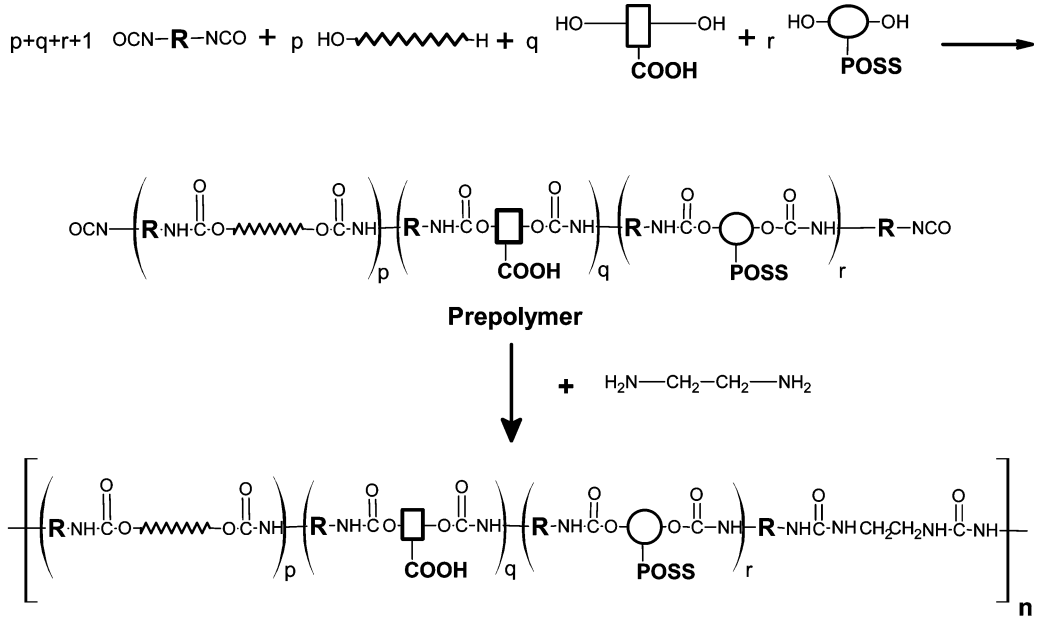

Table 1. Composition and Intrinsic Viscosities of Polyurethane POSS-Modified Samples

sample	PTMG soft phase % (M_n)	IPDI % (w/w)	POSS % (w/w)	[η] (dL/g)
A	55.4 (1000)	35.2	0	0.485
A6	52.2 (1000)	32.8	5.8	0.470
A10	49.1 (1000)	31.0	9.4	0.350
A20	35.6 (1000)	34.2	18.8	n.d.
B	65.5 (2000)	25.3	0	0.580
B10	56.1 (2000)	25.6	9.2	0.450

(glass, PTFE plates) and dried at room temperature for 24 h and then in an air-forced oven at +50 °C for 72 h in order to obtain specimens suitable for the subsequent characterization.

Molecular and Structural Characterization. The end of polymerization was monitored by FTIR spectroscopy with a Nexus ThermoNicolet instrument (16 scans, resolution 4 cm^{-1}), by smearing one or two drops of dispersion between CaF_2 disks and monitoring the disappearance of free NCO band at 2260 cm^{-1}. Molecular weight distribution of prepolymers were measured by GPC at +30 °C (THF, polystyrene calibration standards) with a Waters equipment and RI detector. Prepolymer samples were first derivatized with methanol in order to end-cap the isocyanates, coagulated with diluted HCl, dried, and then dissolved in THF for analysis. Final polyurethanes were only partially soluble in THF; their molecular weights were estimated by intrinsic viscosity measurements in DMF with calibrated capillary glass viscometers at +40 °C. Wide-angle X-ray diffraction experiments (XRD) were carried out on POSS powder and on 500 μm thick PU films with a Philips PW 1710 diffractometer in reflectance mode, with Cu Kα radiation (λ = 1.541 78 Å), scanning from $2\theta = 2°$ to 40° with step size 0.02 and time per step 4 s.

Thermal Analysis. Differential scanning calorimetry (DSC) was carried out with a Mettler-Toledo TA3000 instrument, indium and *n*-hexane calibrated, with the following thermal cycles: heating from +20 to +150 °C at 20 °C/min, quenching at −150 °C, and reheating from −150 to +150 °C at 20 °C/

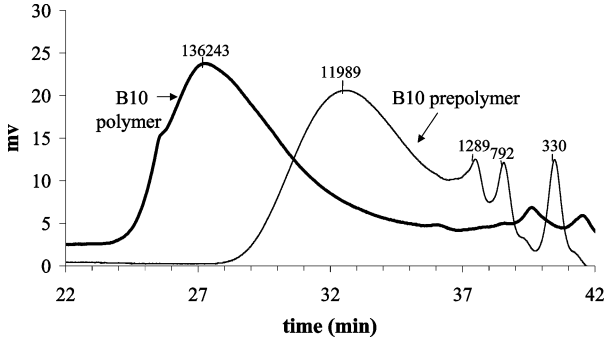

Figure 1. Example of raw GPC chromatograms (sample B10).

min. The glass transition T_g was calculated as inflection in the ΔC_p jump after the second scan.

Dynamic Rheological Measurements. Dynamic mechanical spectra were obtained from cylindrical 500 μm thick samples in shear-sandwich mode using a Mettler-Toledo DMA/SDTA 861^e dynamic mechanical analyzer in dynamic scans from −100 to +130 °C, frequency 1 Hz, and deformation ≤0.3%. Dynamic rheological measurements in the temperature range from +150 to +200 °C were performed with a Rheometrics Scientifics DSR 200 stress controlled rheometer, with a dynamic temperature ramp program, frequency 1 Hz, operating in autostress adjustment mode in order to keep deformation <4%. The curves obtained from the two instruments were overlapped in order to obtain the dynamic modulus−T curve from −100 to +200 °C.

Surface Measurements. Static contact angle measurements with bidistilled water and highest purity diiodomethane were carried out with a Dataphysics OCA 20 instrument. PU films about 2−5 μm thick were bar-coated on well-cleaned glass substrates, air-dried for 24 h at ambient temperature, and oven-dried at +50 °C for 1 h. About 20−30 independent measurements were carried out, and the results were expressed as mean value ±2 standard deviation.

Results and Discussion

Composition and intrinsic viscosities [η] of polyurethanes synthesized are shown in Table 1. All samples are in a strict sense poly(urethane−urea)s since they come from chain extensions of NCO-terminated prepolymers with a diamine. GPC analyses of prepolymer samples just before chain extension step showed an apparent absence of peaks corresponding to the free POSS macromonomer, occurring at retention time = 37.98 min (M = 830 according to PS calibration) in our conditions. This result agrees with the chemical titration of the prepolymer. Therefore, the diol functionalized nanofiller, which is perfectly soluble in THF, has a sufficiently high chemical reactivity to be easily copolymerized during the ionomeric prepolymer formation at high concentration. Unfortunately, most chain extended polyurethanes were only partially soluble in THF, and therefore GPC chromatograms could not be used as a reliable measurement of molecular weight. Polyurethanes based on PTMG 2000 showed a better solubility, likely because of the lower content of urea linkages. As an example, Figure 1 shows the raw GPC chromatograms of B10 prepolymer and final polymer (analyzed after filtration of the solution), essentially confirming the absence of free POSS monomer (labeled peaks corresponds to molecular weights relative to PS calibration). Molecular weights were also estimated by intrinsic viscosity measurements in DMF. From Table 1 examination, it appears that [η] is somewhat lower for the POSS-containing structures. This could be due to an effect of composition on Mark−Houwink parameters or to the fact that polyurethanes containing POSS have a lower molecular weight.

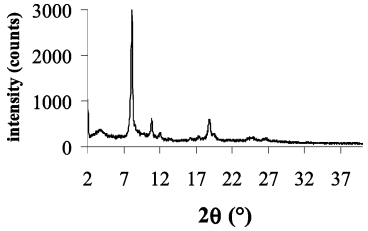

Figure 2. XRD pattern of POSS diol macromonomer.

Table 2. Features of Main XRD Reflections from POSS-Diol Macromonomer

2θ (deg)	d-spacing (Å)	peak half-height width (deg)	peak intensity (counts)
8.1	10.85	0.26	2840
10.8	8.15	0.25	437
12.1	7.31	n.d.	137
18.8	4.71	0.33	449

All the aqueous dispersions obtained were stable (no settling) for at least 6 months at ambient temperature, except for sample A20 containing the highest level of POSS macromer incorporated in the prepolymer. That sample showed also very poor film-forming properties and was not furtherly characterized, except for XRD analysis.

Figure 2 shows the XRD pattern of the POSS macromonomer, while Table 2 reports numerical values of the main reflections. The position of main reflections reported in Table 2 concerning our isobutyl-POSS are in close agreement with the XRD study carried out by Waddon and Coughlin[42] on a quite differently substituted structure, i.e., a cyclopentyl-substituted POSS bearing one norbornyl functional group. According to the classical works on POSS structure,[39,42,43] the crystallographic structure is described with a rhomboedral or hexagonal cell. The Miller indices can be attributed as reported in ref 42, in particular being the most intense reflection at 2θ = 8.1° indexed as 101.

For a hexagonal cell, interplanar distances are related to Miller indices by

$$d_{hkl} = \frac{1}{\sqrt{(4/3a^2)(h^2 + k^2 + hk) + \frac{l^2}{c^2}}} \qquad (1)$$

After refinement analysis, the peaks fitting according to eq 1 gave the other two fundamental hexagonal cell parameters, calculated as a = 16.30 Å and c = 17.24 Å. Such results are in quite good agreement with the structure of cyclopentyl-substituted POSS reported in ref 42.

Figures 3 and 4 show the XRD patterns for all polyurethanes. All the samples show two broad peaks as background centered at about 18° and 6°, which could be attributed to the amorphous polyether phase and to hard−soft type interactions[40] in analogy to other conventional PU systems.[44] It is interesting to observe that all POSS-modified samples show some residual crystallinity in form of 101 reflection at about 8°, even if the intensity of the peak is very small in the case of A6 polymer. This fact would mean that POSS cages maintain a relevant self-assembling ability even when copolymerized by a predominantly statistical process, with formation of nanocrystal phases. Interestingly enough,

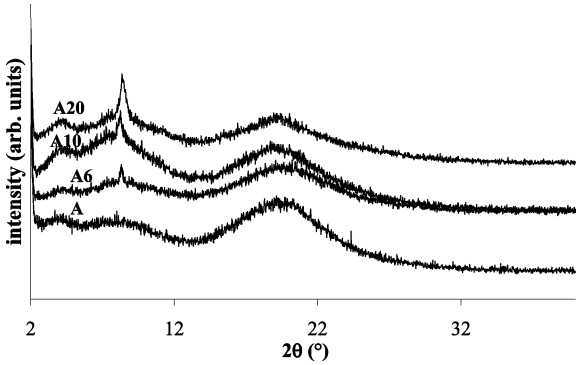

Figure 3. XRD patterns of PU1000 series (samples A, A6, A10, A20).

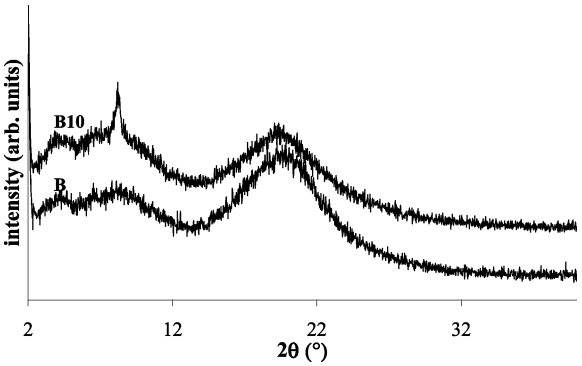

Figure 4. XRD patterns of PU2000 series (samples B, B10).

an effect of sample processing on crystallinity was observed only on sample A6 (lowest POSS content). In particular, the 101 reflection disappeared if the cast dispersions were immediately dried in oven at high temperature and then analyzed. This suggests a kinetic limitation on POSS crystallization with small nanofiller content. On the other hand, crystalline peaks were always present in samples containing 10% of POSS, confirming the findings reported by Fu et al.[38−40] on segmented elastomeric polyurethanes. Although crystalline reflections are weak in polyurethanes, the Scherrer rule can be tentatively applied in order to estimate the average thickness (L) of crystalline aggregates:

$$L = \frac{K\lambda}{\beta \cos \theta} \tag{2}$$

where K is a constant $\cong 0.9$, λ is the wavelength used, and β is the half-width (in rad) of the reflection of concern. As a first approximation, contribution of paracrystalline distortion was not considered. Application of eq 2 gave $L = 38.0$ nm for the POSS-diol crystal, whereas in the polyurethane polymer when the crystalline peak is present as in samples A10 or B10 it corresponds to L about 20 nm. (A larger error has to be expected in the last case due to the low intensity of the 101 reflection.) Therefore, the dimensions of crystalline aggregates in the polyurethanes are smaller than in their precursor, as expected.

DSC analysis of samples detected only the soft phase T_g of the polyether phase, without evidence of other higher temperature hard phase thermal transitions. Values are reported in Table 3. By increasing the POSS fraction in the polymer, the T_g is slightly shifted at higher temperatures. This effect was already reported[40,45−46] and interpreted as a consequence of cohesive interactions like hydrogen bonding between the siloxane cage and polar groups in the macromolecular chain. In our case it seems always present independently on the crystallization of POSS structures.

Table 3. Some Data about Thermal and Dynamic Rheological Characterization of PU Polymers

sample	T_g by DSC (°C)	$G'_{20°C}$ (MPa)	$G'_{100°C}$ (MPa)	tan δ maxima (°C)	T crossover (°C)
A	−48.2	50.5	1.0	+177	+157
A6	−46.0	37.0	0.7	+177	+156
A10	−41.0	55.4	0.7	+172	<+140
B	−72.7	13.2	1.6	+186	+158
B10	−66.0	32.6	2.9	+175	+152

Dynamic properties of some PU films are shown in Figures 5a,b and 6a,b for polyurethanes from PTMG 1000 and 2000, respectively. G' and tan δ vs T trends were obtained by overlapping curves from dynamic mechanical analysis and rotational rheometry. Dynamic curves obtained from the two different instruments nicely fit and allow a reliable estimation of viscoelastic behavior of samples in quite a wide temperature range. In the PU 1000 series the introduction of POSS macromers shows an apparently unclear effect in the temperature range comprised between the soft phase T_g (below −50 °C) and about +100 °C. For example, G' at 20 °C passes from 50.5 to 37.0 MPa (POSS 6%) and 55.4 MPa (POSS 10%). It should be noted that in some other cases introduction of POSS macromers in a copolymer structure did not promote an enhancement in mechanical properties.[25] This behavior was explained by considering that POSS cages are typically large and may disturb cohesive interchain interactions or reduce the degree of crystallinity.

The reinforcing effect is more relevant for the PU 2000 series, for which the $G'_{20°}$ value increases more than 100%. This could be due to a better crystalline aggregation within the polyurethane hard phases.

Some other differences are evident in both the low- and high-temperature regions. Differences in G' below the soft phase T_g are likely of scarce relevance in our case, since it is known that shear-sandwich clamping mode is inadequate to evaluate moduli of glassy polymers with $G > 1$ GPa.[47] On the other hand, the different behavior at high temperature seems more interesting to be discussed. The POSS-based polymers undergo to a softening, broad transition at T comprised between +60 and +100 °C, as shown by a clear decrease in G' corresponding to a broad shoulder in the tan δ curve. The nature of this thermal effect if unclear also because no transition at the DSC analysis is evident within that temperature range. However, above that transition G' is of the order of 10^0 Pa for all samples, therefore typical of the rubbery plateau. By analogy to other PU systems, it could be attributed to the hard phase T_g; this transition is too broad to discuss an effect of POSS introduction, if any. Anyway, it should be noted that in sample B10 the storage modulus is significantly raised, as found for other POSS reinforced systems in the rubbery plateau.[8] The strong drop in G' and sharp peak in tan δ at $T > +150$ °C should be attributed to the α-relaxation of the polymers. It should indicate the terminal flow region of the polymers. The maxima of tan δ peaks are slightly shifted toward lower temperatures in POSS-based PU. Another effect to be considered is the decrease in tan δ peak intensity in POSS-modified polymers. To give a summary of rheological results, Table 3 reports some numerical data including the value of crossover temperature. The crossover

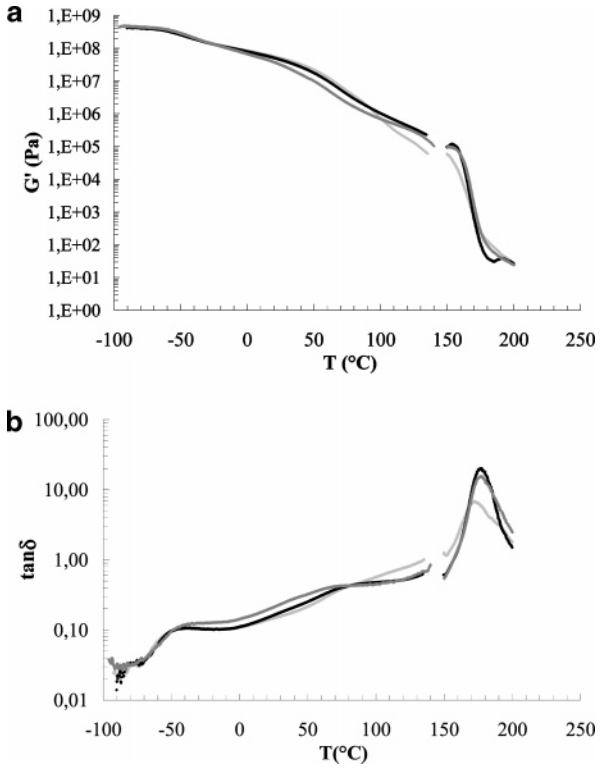

Figure 5. Dynamic rheological properties of PU1000 series: (a) $G'-T$ curves (black line, sample A; gray line, sample A6; light gray line, sample A10); (b) tan $\delta-T$ curves (black line, sample A; gray line, sample A6; light gray line, sample A10).

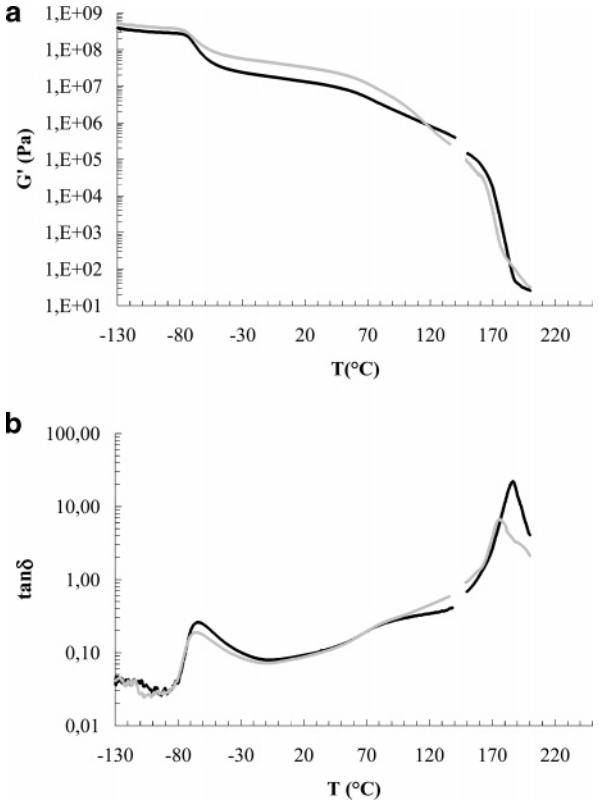

Figure 6. Dynamic rheological properties of PU2000 series: (a) $G'-T$ curves (black line, sample B; light gray line, sample B10); (b) tan $\delta-T$ curves (black line, sample B; light gray line, sample B10).

temperature indicates the condition at which $G'' = G'$, meaning that thermal motion and shear stress cause the disengagement of entanglements. At $T > T_{\text{crossover}}$ the viscous character prevails over the elastic one. Crossover occurs at lower temperature for POSS containing PU; again, it might be an indication of lower molecular weight in nanostructured samples.

Finally, surface behavior was investigated through measurements of contact angles against water and diiodomethane. Results are shown in Figure 7, where it appears that incorporation of even a small amount of POSS macromer strongly enhances the contact angles of the coated surface against both liquids. Results are very reliable and reproducible as shown by the small confidence interval on the graph. Contact angle data (cos Θ) were used in order to calculate the polymer surface energy γ_s in its polar (γ_s^p) and dispersive (γ_s^d) components according to the Wu's harmonic mean approximation:[48]

$$\gamma_{sl} = \gamma_s + \gamma_l - \frac{4\gamma_l^d\gamma_s^d}{\gamma_l^d + \gamma_s^d} - \frac{4\gamma_l^p\gamma_s^p}{\gamma_l^p + \gamma_s^p}$$

$$\gamma_s = \gamma_{sl} + \gamma_l \cos\Theta \qquad (3)$$

where γ_{sl} is the interfacial tension of the system. Calculations are reported in Table 4. It appears that the total surface energy of polyurethanes is in any case reduced from more than 40 to about 30 mN/m. In particular, the polar component is very sensitive to the presence of even few POSS percentages. This would mean the POSS nanostructures screen the polar groups like urethanes and carboxyls and are preferentially oriented air-side. So far, very few examples were reported about the effect of polyhedral oligomeric silsesquioxane nanostructures in enhancing surface properties of a polymer.[49,50] This issue is going to be investigated in more detail in a future paper.

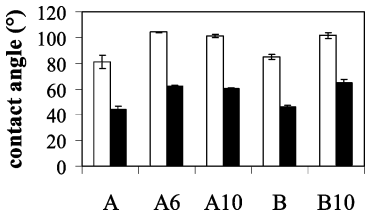

Figure 7. Static contact angles against H_2O (white) and CH_2I_2 (black).

Table 4. Surface Energy Dispersive (γ_s^d) and Polar (γ_s^p) Components at $T = 25$ °C Calculated According to Wu

sample	γ_s^d (mN/m)	γ_s^p (mN/m)
A	34.8	8.7
A6	28.2	1.2
A10	28.5	2.1
B	34.0	7.2
B10	26.1	2.6

Conclusions

It has been shown the OH-functionalized POSS macromonomers can be easily incorporated by copolymerization within a classical ionomeric polyurethane structure. Both synthetic procedures and water dispersibility are not affected by the introduction of reactive POSS up to a level of 10%. POSS structures maintain a relevant self-assembling ability generating nanocrystalline domains with dimensions of the order of 20 nm. These structures have a slight effect on viscoelastic properties and no effect on appearance, since the coated

polymer films remain glossy and transparent. Interestingly, POSS nanostructured surfaces showed lower wettability and significant reduction in polar surface energy component even with a limited POSS modification. This effect may be due to both a stratification of apolar components of the coating close to polymer−air interface and a topographical change of the surface due to formation of nanosized structures.

References and Notes

(1) Lichtenhan, J. D. *Comm. Inorg. Chem.* **1995**, *17*, 115−130.
(2) Schwab, J. J.; Lichtenhan, J. D. *Appl. Organomet. Chem.* **1998**, *32*, 707−713.
(3) Laine, R. M.; Zhang, C.; Sellinger, A.; Viculis, L. *Appl. Organomet. Chem.* **1998**, *12*, 715−723.
(4) Shockey, E. G.; Bolf, A. G.; Jones, F.; Schwab, J. J.; Chaffee, K. P.; Haddad, T. S.; Lichtenhan, J. D. *Appl. Organomet. Chem.* **1999**, *13*, 311−327.
(5) Li, G.; Wang, L.; Ni, H.; Pittman, C. U. J. *Inorg. Organomet. Polym.* **2002**, *11*, 123−154.
(6) Giannelis, E. P.; Shah, D.; Schmidt, D. *Curr. Opin. Solid State Mater. Sci.* **2002**, *6*, 205−212.
(7) Haddad, T. S.; Lichtenhan, J. D. *Macromolecules* **1996**, *29*, 7302−7304.
(8) Romo-Uribe, A.; Mather, P. T.; Haddad, T. S.; Lichtenhan, J. D. *J. Polym. Sci., Part B: Polym. Phys.* **1998**, *36*, 1857−1872.
(9) Xu, H.; Kuo, S. W.; Lee, J. S.; Chang, F. C. *Polymer* **2002**, *43*, 5117−5124.
(10) Haddad, T. S.; Viers, B. D.; Phillips, S. H. *J. Inorg. Organomet. Polym.* **2002**, *11*, 155−164.
(11) Zheng, L.; Kasi, R. M.; Farris, R. J.; Coughlin, E. B. *J. Polym. Sci., Part A: Polym. Chem.* **2002**, *40*, 885−891.
(12) Fu, B. X.; Lee, A.; Haddad, T. S. *Macromolecules* **2004**, *37*, 5211−5218.
(13) Lichtenhan, J. D.; Otonari, Y. A.; Carr, M. J. *Macromolecules* **1995**, *28*, 8435−8437.
(14) Pyun, J.; Matyiaszewsi, K.; Wu, J.; Kim, G. M.; Chun, S. B.; Mather, P. T. *Polymer* **2003**, 2739−2750.
(15) Zhang, W.; Fu, B. X.; Seo, Y.; Schrag, E.; Hsiao, B.; Mather, P. T.; Yang, N. L.; Xu, D.; Ade, H.; Rafailovich, M.; Sokolov, J. *Macromolecules* **2002**, *35*, 8029−8038.
(16) Kopesky, E. T.; Haddad, T. S.; Cohen, R. E.; McKinley, G. H. *Macromolecules* **2004**, *37*, 8992−9004.
(17) Lee, A.; Lichtenhan, J. D. *Macromolecules* **1998**, *31*, 4970−4974.
(18) Lee, A.; Lichtenhan, J. D. *J. Appl. Polym. Sci.* **1999**, *73*, 1993−2001.
(19) Li, G. Z.; Wang, L.; Toghiani, H.; Daulton, T. L.; Koyama, K.; Pittman, C. U. *Macromolecules* **2001**, *34*, 8686−8693.
(20) Ni, Y.; Zheng, S.; Nie, K. *Polymer* **2004**, *45*, 5557−5568.
(21) Strachota, A.; Kroutilova, I.; Kovarova, J.; Matejka, L. *Macromolecules* **2004**, *37*, 9457−9464.
(22) Matejka, L.; Strachota, A.; Plestil, J.; Whelan, P.; Steinhart, M.; Slouf, M. *Macromolecules* **2004**, *37*, 9449−9456.
(23) Tsuchida, A.; Bolln, C.; Sernetz, F. G.; Frey, H.; Muhlhaupt, R. *Macromolecules* **1997**, *30*, 2818−2824.
(24) Mather, P. T.; Jeon, H. G.; Romo-Uribe, A.; Haddad, T. S.; Lichtenhan, J. D. *Macromolecules* **1999**, *32*, 1194−1203.
(25) Zheng, L.; Farris, R. J.; Coughlin, E. B. *Macromolecules* **2001**, *34*, 8034−8039.
(26) Waddon, A. J.; Zheng, L.; Farris, R. J.; Coughlin, E. B. *Nano Lett.* **2002**, *2*, 1149−1155.
(27) Zhang, L.; Waddon, A. J.; Farris, R. J.; Coughlin, E. B. *Macromolecules* **2002**, *35*, 2375−2379.
(28) Leu, C. M.; Reddy, G. M.; Wie, K. H.; Shu, C. F. *Chem. Mater.* **2003**, *15*, 2261−2265.
(29) Huang, J.; He, C.; Xiao, Y.; Mya, K. Y.; Dai, J.; Siow, Y. P. *Polymer* **2003**, *44*, 4491−4490.
(30) Tamaki, R.; Choi, J.; Laine, R. M. *Chem. Mater.* **2003**, *15*, 793−797.
(31) Phillips, S.; Haddad, T. S.; Tomczak, S. J. *Curr. Opin. Solid State Mater. Sci.* **2004**, *8*, 21−29.
(32) Gonzalez, R. I.; Phillips, S. H.; Hoflund, G. B. *J. Spacecraft Rockets* **2000**, *37*, 463−467.
(33) Gilman, J. W.; Schlitzer, D. S.; Lichtenhan, J. D. *J. Appl. Polym. Sci.* **1996**, *60*, 591−596.
(34) Gao, F.; Tong, Y.; Schricker, S. R.; Culbertson, B. M. *Polym. Adv. Technol.* **2001**, *12*, 355−360.
(35) Tegou, E.; Bellas, V.; Gogolides, E.; Argitis, P. *Microelectr. Eng.* **2004**, *73*−*74*, 238−243.
(36) Kickelbick, G. *Prog. Polym. Sci.* **2003**, *28*, 83−114.
(37) Neumann, D.; Fisher, M.; Tran, L.; Matisons, J. G. *J. Am. Chem. Soc.* **2002**, *124*, 13998−13999.
(38) Fu, B. X.; Hsiao, B. S.; White, H.; Rafailovich, M.; Mather, P. T.; Jeon, H. G.; Phillips, S.; Lichtenhan, J. D.; Schwab, J. J. *Polym. Int.* **2000**, *49*, 437−440.
(39) Fu, B. X.; Hsiao, B. S.; Pagola, S.; Stephens, P.; White, H.; Rafailovich, M.; Sokolov, J.; Mather, P. T.; Jeon, H. G.; Phillips, S.; Lichtenhan, J. D.; Schwab, J. J. *Polymer* **2000**, *42*, 599−611.
(40) Fu, B. X.; Zhang, W.; Hsiao, B. S.; Rafailovich, M.; Sokolov, J.; Johansson, G.; Sauer, B. B.; Phillips, S.; Balnski, R. *High Perform. Polym*. **2000**, *12*, 565−571.
(41) Dieterich, D. *Prog. Org. Coat.* **1981**, *9*, 281−340.
(42) Waddon, A. J.; Coughlin, E. B. *Chem. Mater.* **2003**, *15*, 4555−4561.
(43) W. H.; Domicone, J. J.; Gilkey, J. W. *J. Am. Chem. Soc.* **1955**, *77*, 4248.
(44) Bonart, R. *J. Macromol. Sci., Part B* **1968**, *2*, 115.
(45) Xu, H.; Kuo, S. W.; Lee, J. S.; Chang, F. C. *Macromolecules* **2002**, *35*, 8788−8793.
(46) Xu, H.; Kuo, S. W.; Huang, C. F.; Chang, F. C. *J. Appl. Polym. Sci.* **2003**, *91*, 2208−2215.
(47) Gradin, P.; Howgate, P. G.; Selden, R. In *Comprehensive Polymer Science*; Booth, C., Price, C., Eds.; Pergamon Press: Oxford, 1989; Vol. 2, pp 554−555.
(48) Wu, S. *J. Polym. Sci., Part C* **1971**, *34*, 19−22.
(49) Mabry, J. M.; Marchant, D.; Viers, B.; Ruth, N. P.; Barker, S.; Schaefler, C. E. *SAMPE 2004* **2004**, *49*, 1316−1328.
(50) Suresh, S.; Zhou, W.; Spraul, B.; Laine, R. M.; Ballato, J.; Smith, D. W. *J. Nanosci. Nanotechnol.* **2004**, *4*, 250−253.

MA047304G